RHPN1-AS1 promotes ovarian carcinogenesis by sponging miR-485-5p and releasing TPX2 mRNA

SHOUBIN CUI* and CUI LI*

Department of Gynaecology and Obstetrics, Yantai Affiliated Hospital of Binzhou Medical University, Yantai, Shandong 264100, P.R. China

Received August 13, 2020; Accepted February 5, 2021

DOI: 10.3892/or.2021.8062

Abstract. Long non-coding RNAs (lncRNAs) play a crucial role in cancer development. However, researchers have yet to identify the underlying association between lncRNAs and ovarian cancer (OC). The aim of the present study was to examine the effect of lncRNA RHPN1-AS1 (RHPN1-AS1) on OC cells and tissues. Reverse transcriptase-quantitative PCR (RT-qPCR) was utilized to quantify RHPN1-AS1, miR-485-5p, and *TPX2* mRNA expression in samples with OC. Luciferase-reporter assay, RNA immunoprecipitation (RIP) assay, and RNA pull-down assay were then employed to validate the target relationship among RHPN1-AS1, miR-485-5p and *TPX2*. Cell Counting Kit-8, BrdU, wound-healing, cell-adhesion, and flow cytometry assays were also employed to assess cell viability, proliferation, migration, adhesion and apoptosis, respectively, in SKOV3 and OVCAR3 cell lines. Findings revealed that RHPN1-AS1 demonstrated a higher expression level in OC cell lines and tissues. In addition, RHPN1-AS1 enhanced the adhesion, proliferation and migration of OC cell lines but decreased apoptosis of OC cells. It was also observed that the relationship between RHPN1-AS1 and miR-485-5p was negative and that RHPN1-AS1 could sponge miR-485-5p to regulate the proliferation, apoptosis, adhesion, and migration abilities of OC cells. Moreover, *TPX2* was targeted by miR-485-5p and was significantly overexpressed in OC cell lines and tissues. Experimental investigations also revealed that *TPX2* promoted the proliferation, adhesion, and migration of OC cells but suppressed the apoptosis of SKOV3 and OVCAR3 cells. In summary, RHPN1-AS1 played a tumor promotive role by sponging miR-485-5p to increase *TPX2* expression in OC tumorigenesis.

Correspondence to: Dr Shoubin Cui, Department of Gynaecology and Obstetrics, Yantai Affiliated Hospital of Binzhou Medical University, 717 Jinbu Street, Muping, Yantai, Shandong 264100, P.R. China
E-mail: cuishoubin98@163.com

*Contributed equally

Key words: RHPN1-AS1, miR-485-5p, *TPX2*, ovarian cancer

Introduction

Ovarian cancer (OC) can be referred to as the malignancy growth that originates from the ovaries. In 2018, this invasive cancer has claimed the lives of approximately 185,000 individuals worldwide (1). In the last decade, there has been a significant increase in individuals succumbing to OC in Asia, including China (2). The current five-year survival rate of OC varies from 29 to 49%, depending on the severity of the tumor (3). Owing to the complex histological classification of OC, the molecular pathogenesis is somewhat complicated. Findings have shown that the functional mutations of the *TP53* gene account for the occurrence of OC, especially high-grade ovarian carcinoma (3,4). Additionally, the recurrent somatic mutations in the gene locus of NF1, BRCA1, BRCA2, RB1, and CDK12 were found to be associated with OC pathogenesis (5). Although treatment methods such as surgery, chemotherapy and radiation therapy have been used to combat the spread of OC, OC patients are encumbered with poor prognosis. Therefore, the identification of new biomarkers for the diagnosis and treatment of OC is imperative.

Several reports in the literature have confirmed that long non-coding RNAs (lncRNAs) contribute to the growth of malignant tumors (6). Also known as C8orf51, RHPN1-AS1 is located at chromosome 8q24.3, and it contains 1 exon (7). This RNA was found to be over-expressed in uveal melanoma in 2017 (7), and it has been verified as a significant tumor promoter in a number of malignant cancers such as gastric cancer, hepatocellular carcinoma, breast cancer, colorectal cancer, glioma, and cancer of the head and neck (8-14). However, research has not explored the impact of RHPN1-AS1 in OC development. The present study aimed to investigate the impact and the underlying mechanism of RHPN1-AS1 on OC.

In the last decade, evidence has demonstrated that a large number of small RNAs play a considerable role in carcinogenesis (15). More specifically, miRNAs are widely reported to be associated with the tumorigenesis of multitype malignancies (16-18). A member of miRNAs, miR-485-5p was found to play tumor-inhibitory roles in breast cancer, hepatocellular carcinoma, cervical cancer, melanoma, lung cancer, oral tongue squamous cell carcinoma, osteosarcoma, glioblastoma, colorectal cancer, esophageal cancer, and thyroid carcinoma (19-31). Another study confirmed that miR-485-5p could inhibit the spread of OC by regulating

UCA1 (32). It was also reported that miR-485-5p could serve as a sponging target of RHPN1-AS1 in the pathogenesis of hepatocellular carcinoma (33,34). Findings of those studies confirmed the effects of RHPN1-AS1/miR-485-5p on OC progression. Nevertheless, to the best of our knowledge, no study has explored the upstream regulator of miR-485-5p in OC or investigated whether miR-485-5p could be regulated by RHPN1-AS1 in OC cells.

Located on human chromosome 20q11.21 with an exon count of 18, targeting protein for Xklp2 (*TPX2*) can encode a microtubule-related protein (35). In the early stage of mitosis, *TPX2* is the downstream of Ran-GTP, and it participates in spindle formation (36). *TPX2* is also regulated at all stages of the cell cycle, and *TPX2* was downregulated at the G1-S transition boundary and upregulated as the cell cycle progressed into S and G2 phases (37). Therefore, *TPX2* may provide insights into tumor cell proliferation. Evidence documented in the literature suggested that *TPX2* was upregulated in such tumors as cervical cancer, lung cancer, pancreatic ductal adenocarcinomas, bladder cancer, OC and colon cancer (38-44). More importantly, a recent study revealed that miR-485-3p could suppress colorectal cancer by targeting *TPX2* (45). The above-mentioned results emphasize the significance of miR-485 and *TPX2* in cancer development. However, no studies have confirmed whether *TPX2* could be regulated by miR-485-5p in OC cells and whether the RHPN1-AS1/miR-485-5p/*TPX2* axis could contribute to OC pathogenesis.

The aim of the current study was to demonstrate the effect of the RHPN1-AS1/miR-485-5p/*TPX2* axis on OC. It was hypothesized that RHPN1-AS1 acted as a tumor promoter in OC by interacting with miR-485-5p to increase *TPX2*. The results of this study may provide insights into OC diagnoses and treatments.

Materials and methods

Bioinformatics analysis. GSE119056 and GSE23392 downloaded from the GEO DataSets were the mRNA expression profiles involving ovarian cancer. GEPIA database (http://gepia.cancer-pku.cn/index.html) is a public database showing the differentially expressed genes (DEGs) or lncRNAs in ovarian cancer. With P-value <0.01 and |$\log_2$ fold change| (|logFC|)≥1.5, DEGs were screened out from GEPIA, GSE119056 and GSE23392. The STRING database (https://string-db.org/) was then used to construct the interaction network for the screened DEGs with the medium confidence (0.400) of interaction score. TargetScan and ENCORI Starbase were finally employed to predict the miRNAs targeting *TPX2* and the miRNAs sponged by RHPN1-AS1, respectively.

Patients. OC tissues and adjacent normal ovarian tissues were collected from 37 OC patients at the Yantai Affiliated Hospital of Binzhou Medical University (China). The relevant characteristics are shown in Table I. The collection and use of the clinical tissues were performed based on the ethical standards set out in the Helsinki Declaration. All participants signed the informed consent forms, and this study was approved by the Ethics Committee of the Yantai Affiliated Hospital of Binzhou Medical University.

Table I. Baseline characteristic of 37 patients with ovarian cancer.

Total no. of patients=37	No. (%)
Age at diagnosis (years)	
>55	20 (54.05)
≤55	17 (45.95)
Tumor size (cm)	
≤10	23 (62.16)
>10	14 (37.84)
Tumor type	
Invasive	17 (45.95)
Borderline	15 (40.54)
Unknown	5 (13.51)
FIGO stage	
I/II	24 (64.86)
III/IV	13 (35.14)
Pathological grade	
G1+G2	21 (56.76)
G3	16 (43.24)

RNA isolation and RT-qPCR. RNAs were extracted from tissues and cells with the miRcute miRNA Isolation Kit (Tiangen). This extraction was carried out according to the manufacturer's instructions. The miRcute miRNA First-strand cDNA Synthesis Kit (Tiangen) and the PrimeScript™ RT reagent Kit (Takara) were used to perform miRNA reverse transcription and lncRNA and mRNA reverse transcription, respectively. Then, the expression of miR-485-5p, RHPN1-AS1 and mRNA of *TPX2* in OC samples was analyzed using TB Green Premix Ex Taq II (Takara) with 95˚C 30 sec denaturation, followed by 40 cycles at 95˚C for 5 sec and 60˚C for 30 sec. The reference gene for RHPN1-AS1 and *TPX2* mRNA was *GAPDH*, while the reference gene for miR-485-5p was *U6*. Primers were obtained from GeneCopoeia, and the corresponding sequences are listed in Table II. The $2^{-\Delta\Delta Ct}$ method (46) was used to estimate LncRNA, miRNA and mRNA expressions. This experiment was repeated three times.

Cell culture. Biological materials were purchased from the Bena Culture Collection (Beijing), such as CaOV4, OVCAR3, CaOV3, SKOV3, and HOSEpiC (human ovarian surface epithelial cells) cell lines. A mixture containing fetal bovine serum (10%) and DMEM (Dulbecco's modified Eagle's medium) was utilized to culture CaOV3. DMEM containing 4 mM L-glutamine and sodium pyruvate and 10% FBS was used to culture OVCAR3 cells. SKOV3 cells were cultured in the McCoy's 5A medium, which contained $NaHCO_3$ (2.2 g/l) and 10% FBS. CaOV4 cells were cultured in L15 medium, which contained 10% FBS. HOSEpiC was kept in the RPMI-1640 medium, which contained 10% FBS. The temperature of the cells was sustained at 37˚C in a humidified air containing 5% CO_2.

Subcellular fractionation. The PARIS™ Kit (Invitrogen; Thermo Fisher Scientific) was used to separate and isolate the

Table II. Primer sequences.

Gene name	Forward primer 5'-3'	Reverse primer 5'-3'
RHPN1-AS1	TGTGAGTCCTCCGACAATGC	AACTTGATGACCAGGAGCCG
miR-485-5p	ACTTGGAGAGAGGCTGGC	AAAAGAGAGGAGAGCCGTGT
U6	AGTAAGCCCTTGCTGTCAGTG	CCTGGGTCTGATAATGCTGGG
TPX2	ATGGAACTGGAGGGCTTTTTC	TGTTGTCAACTGGTTTCAAAGGT
GAPDH	GGAGCGAGATCCCTCCAAAAT	GGCTGTTGTCATACTTCTCATGG

RNA from cytoplasmic and nuclear SKOV3 and OVCAR3 cells. The fractionation buffer was first added to the cells. Then, the cells were centrifuged at 10,000 x g, for 5 min at 4˚C. The cell supernatant was then obtained, followed by the lysis of the pellet with a disruption buffer. The RNAs in the cell supernatant containing cytoplasmic lysate and nuclear lysate were later isolated with Lysis/Binding Solution. Subsequently, the cell lines were treated with 100% ethanol. The expression level of RHPN1-AS1, U2 (served as a nuclear control) and GAPDH (served as a cytoplasmic control) was determined using reverse transcription-quantitative PCR (RT-qPCR). This experiment was repeated three times.

Cell transfection. Genomics products were purchased from GeneCopoeia (Guangzhou), including miRNA mimic negative control, miRNA inhibitor negative control and small interference RNA negative control, pcDNA3.1 empty vector, pcDNA3.1-*TPX2* overexpression vector, si-*TPX2* (*TPX2* small interference RNA), miR-485-5p inhibitors, miR-485-5p mimics, and si-RHPN1-AS1 (RHPN1-AS1 small interference RNA). Then, $6x10^4$ OVCAR3 and SKOV3 cell lines were seeded into 6-well plates and cultured overnight at 37˚C before transfection. Lipofectamine 2000 reagent (cat. no. 11668027; Thermo Fisher Scientific) was applied for the transfection of siRNAs, miRNA mimic and miRNA inhibitors into target cells based on the user manual. After 48-h transfection, the cells were collected and the transfection efficiency was detected three times.

Cell viability assessment. Cell viability at 96, 72, 48, and 24 h was measured with CCK-8 (Cell Counting Kit-8). A total of 4,800 cells were subsequently seeded into each well of the 96 plates and cultured at 37˚C after transfection for 24, 48, 72, and 96 h. Next, 10 μl CCK-8 solution was added to each well, followed by incubation at 37˚C for 2 h. Finally, the optical density at 450 nm was read with the aid of a Multiskan FC microplate reader (Thermo Fisher Scientific). This experiment was repeated three times.

Cell proliferation assessment. BrdU assay was utilized to evaluate cell proliferation. After the transfected SKOV3 and OVCAR3 cells ($3x10^4$/ml) were plated into each well of 96-well plates for 24 h, 10 μl/well 5-bromo-2'-deoxyuridine (BrdU) was added to the cells. The cells were then incubated for 4 h. Thymidine analog (Abcam, ab142567) was then added to cells, and the mixture was incubated at 22˚C for 15 min. Finally, the optical density at 450 nm was measured with a Multiskan FC microplate reader (Thermo Fisher Scientific). This experiment was repeated three times.

Cell apoptosis assessment. The transfected cells were collected and rinsed with PBS three times. Following that, $3x10^5$ cells were fixed in cold methanol at 4˚C for 30 min. After washing the cells with PBS three times, 100 μl 1X binding buffer diluted with Annexin V-FITC was added to the fixed cells in the dark for 10 min at 37˚C. Prior to subjecting the cells to flow cytometer (Cytoflex, Beckman Coulter), the cells were stained with 5 μl PI and washed twice with PBS. The flow cytometry (FCM) data were then obtained and analyzed using FlowJo version 7.6.5 software (Tree Star). The rate of cell apoptosis was calculated as the sum of ratio of the top-right (Annexin V^+/PI^+) and the bottom-right (Annexin V^+/PI^-). This experiment was repeated three times.

Wound healing assay. Cells ($2x10^5$/well were plated into 12-well plates until the cells reached 90% confluency. The fused monolayer cells were then scratched with a pipette tip (100 μl), and the exfoliated cells were washed gently with PBS. Subsequently, the cells were cultured in a serum-free medium for 24 h. Using an optic microscope (Leica), the images at 0 and 24 h were captured with x100 magnification to evaluate cell migration. This experiment was repeated three times.

Cell adhesion assessment. Transfected SKOV3 and OVCAR3 cell lines ($5x10^3$ cells) were plated into 96-well plates coated with type I collagen (10 μg/ml). After culturing for 1 h at 37˚C, the culture medium was removed, and the cell wells were rinsed with PBS to remove the floating cells. The adherent cells underwent 4% paraformaldehyde fixation, 0.5% crystal violet staining and dye extraction with sodium citrate methanol solution. The optical density (OD) at 570 nm was measured using a microplate reader. The relative adhesion ability of the blank group was calculated and subjected to statistical analysis. This experiment was repeated three times.

Luciferase reporter assay. The genomics materials for this assay were obtained from GeneCopoeia, such as SEAP (secreted alkaline phosphatase, the internal control) and Gaussia Luciferase (GLuc) reporter gene *pEZX-MT05* with wild-type or mutant RHPN1-AS1-3'UTR or wild-type or mutant *TPX2*-3'UTR. Next, the negative control and miR-485-5p mimic were co-transfected into OVCAR3 and SKOV3 cell lines along with SEAP, and the above Gluc reporter plasmids using Lipofectamine 2000 reagent. The cells collected were lysed with lysis buffer and then transfected for 48 h. The GeneCopoeia's Secrete-Pair™ Dual Luminescence Assay Kit was later used to analyze the relative luciferase activity. The

analysis was performed with a standard microplate reader. The activity ratio of GLuc/SEAP in each group was calculated and compared with other groups. This experiment was repeated three times.

RNA immunoprecipitation (RIP) assay. The EZ-Magna RIP™ RNA-Binding Protein Immunoprecipitation Kit RNA Immunoprecipitation (RIP) Kit was used to perform RIP immunoprecipitation based on the manual protocol. OVCAR3 and SKOV3 cell lines with miR-485-5p mimic transfection or negative-control transfection were lysed in a standard RIP buffer. The cell lysates were then incubated with magnetic beads conjugated with AGO2 (anti-Argonaute2) or anti-IgG (anti-Immunoglobulin G) antibodies served as the negative control for 12 h at 4˚C. After washing the beads with the RIP wash buffer, Proteinase K was used to digest the precipitate by incubating the mixture at 55˚C for 30 min. Subsequently, the total RNAs in the digested supernatant were isolated with phenol: Chloroform: Isoamyl alcohol, which was then reverse-transcribed into cDNA using the kit. Finally, RT-qPCR was used to measure the relative indication of RHPN1-AS1. This experiment was repeated three times.

RNA pull-down assay. This assay was conducted based on the methodology used in the previous report (47). SKOV3 and OVCAR3 cells transfected were seeded into 6-well plates at a concentration of $6x10^5$/well. Subsequently, the cells were incubated for 12 h at 37˚C in humid air filled with 5% CO_2. Then, biotinylated-miR-485-5p mimics and biotinylated-negative controls purchased from RiboBio were transfected into the cultured cells using Lipofectamine 2000 Reagent (Invitrogen; Thermo Fisher Scientific). After 2 days, the cell lysates were collected, sonicated and incubated with streptavidin beads (Life Technologies) for 3 h at 4˚C. The cells were then washed three times with PBS. Subsequently, the RNeasy Mini Kit (Qiagen) was used to elute the bound RNAs. The eluted RNAs were then reverse-transcribed into cDNA, which was then subjected to RT-qPCR to estimate the relative expression of *TPX2*. This experiment was repeated three times.

Western blot assay. The proteins in SKOV3 and OVCAR3 cells were extracted with the RIPA lysis buffer. Next, the Thermo Fisher Scientific Pierce™ BCA Protein Assay Kit was utilized to quantify the concentration of protein in different groups. Then, 20 μg protein was then loaded into 10% SDS-PAGE gel and separated using gel electrophoresis. The separated protein was then transferred onto a PVDF membrane, which was then blocked with 5.0% BSA at 37˚C for 60 min. Subsequently, the primary antibodies against *TPX2* (cat. no. ab252944; Abcam) and GAPDH (cat. no. ab181602, Abcam) were used to incubate the PVDF membranes at 37˚C for 1 h. Subsequently, the cell lines were incubated for 12 h at 4˚C. The Goat Anti-Rabbit IgG H&L secondary antibodies (cat. no. ab205718; Abcam) were used to incubate the PVDF membrane for 1 h at room temperature. Lastly, the ECL Substrate Kit (Abcam) was used for protein blot visualization, which was analyzed with Image-Pro Plus 6.0 produced by Media Cybernetics. This experiment was repeated three times.

Statistical analysis. Three biological repeats were carried out for each experiment. Statistical data were evaluated with GraphPad Prism 8.0 (GraphPad Prism Inc.) and they were presented as mean ± standard deviation (SD). Two-tailed unpaired t-test and one-way or two-way ANOVA with Dunnett's or Tukey's post hoc test were employed for statistical difference analyses between two groups and among multiple groups, respectively. It was assumed that variables with P-values <0.05 were statistically significant.

Results

mRNA and miRNA identification. To identify the most significant genes involved in OC, the GSE119056 and GSE23392 were downloaded from the GEO DataSets. A total of 24 genes were found to be overlapped between the three datasets (Fig. 1A). The 24 genes were then uploaded into the STRING database and an interaction network analysis was constructed. A total of 11 genes were found to be closely associated with each other in the network. Within the network, it was observed that *TPX2* (Fig. 1B) was significantly upregulated (Fig. 1C) in OC and was partly responsible for cancerous growth in OC (44,48,49). However, researchers are yet to study its effect on OC cells. In this study, lncRNA RHPN1-AS1 was evaluated and found to be significantly upregulated in OC according to the data from GEPIA (Fig. 1D) and was regarded as a tumor enhancer in the OC ceRNA system (50,51). Next, TargetScan predicted the miRNAs bound to *TPX2* (Table SI), while ENCORI Starbase predicted the miRNAs sponged by RHPN1-AS1 (Table SII). After intersecting the target miRNAs of RHPN1-AS1 and the target miRNAs of *TPX2*, findings revealed three common miRNAs that could be sponged by RHPN1-AS1 and target *TPX2* mRNA. They included miR-485-5p, miR-6884-5p, and miR-339-5p (Fig. 1E). The effect of miR-485-5p on OC remains unclear, and it was hypothesized that the novel interactome, RHPN1-AS1-miR-485-5p-*TPX2*, may influence OC progression.

RHPN1-AS1 enhanced OC development. The OC tumor tissues obtained from the participants were used to observe the level of RHPN1-AS1. Experimental results confirmed that RHPN1-AS1 upregulated OC tissues by 3-fold in contrast with normal adjacent tissues (Fig. 2A), meaning RHPN1-AS1 is a potential biomarker of OC. To further explore the impact of RHPN1-AS1 on OC, RHPN1-AS1 expression was detected in a normal human ovarian epithelial cell (HOSEpiC) and four typical OC cell lines (SKOV3, CaOV3, OVCAR3 and CaOV4). Findings indicated that the degree of RHPN1-AS1 expression was higher in OC cell lines than in HOSEpiC cell lines (Fig. 2B). The subcellular fractionation location assay was then employed to observe the subcellular location of RHPN1-AS1 in SKOV3 and OVCAR3 cell lines. According to the results of GAPDH and U2, RHPN1-AS1 was found mainly in the cytoplasm (Fig. 2C). Additionally, si-RHPN1-AS1, negative control (NC) and blank control (blank) were transfected into SKOV3 and OVCAR3 cell lines to evaluate the regulatory role of RHPN1-AS1 in OC. To examine the transfection efficiency, RT-qPCR was employed. Data analyses revealed that RHPN1-AS1 in the si-RHPN1-AS1 group was downregulated by 70% compared to the blank group

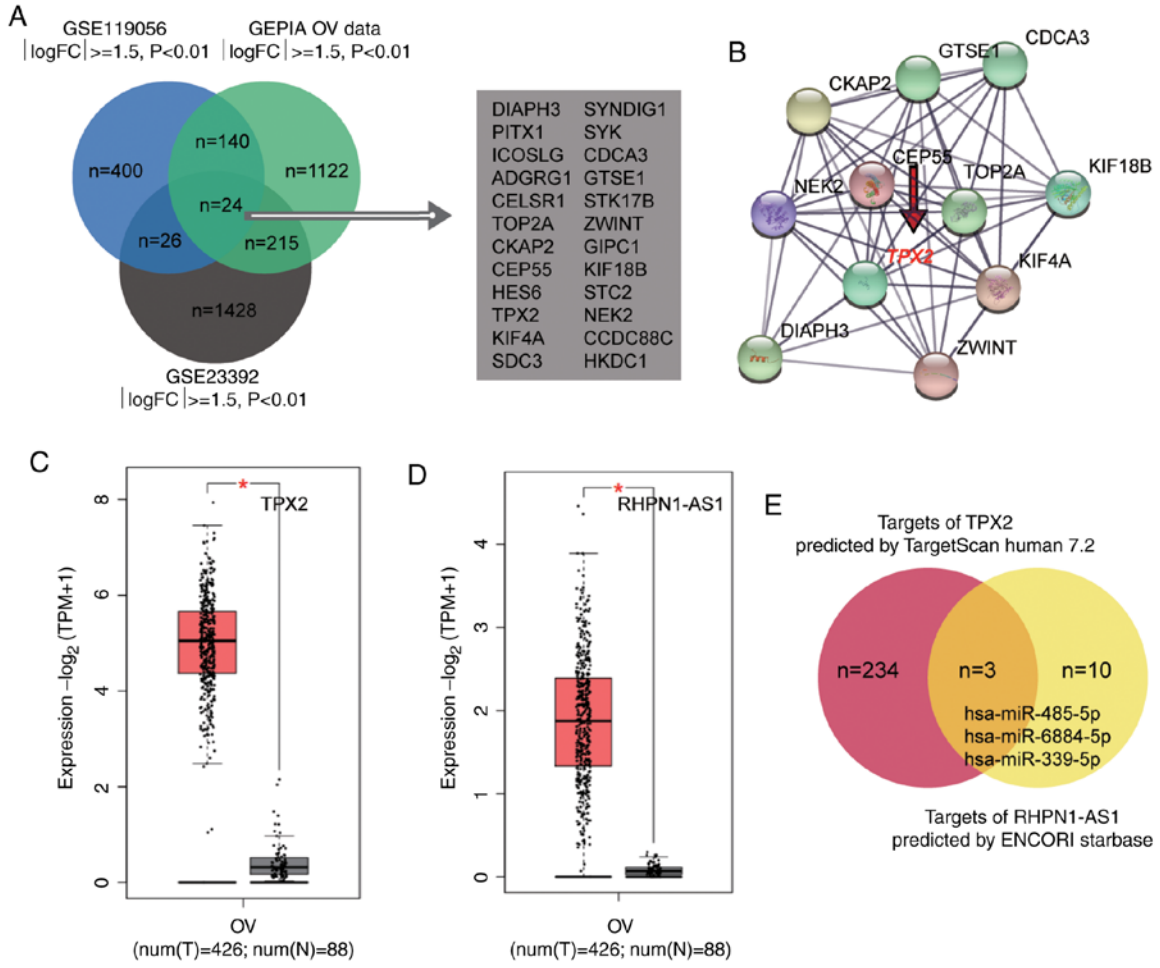

Figure 1. Identification of mRNA and miRNA of interest in this study. (A) The overlapping genes of the significantly upregulated genes from GSE119056 and GSE23392 data series downloaded from GEO database, and those from GEPIA database. (B) The STRING networking results of the 24 overlapping genes from (A). (C) The expression of *TPX2* in ovarian cancer using GEPIA database. *P<0.01. (D) Expression of RHPN1-AS1 in ovarian cancer using GEPIA database. *P<0.01. (E) The common target miRNAs of *TPX2* predicted by TargetScan Human 7.2 and of RHPN1-AS1 predicted by ENCORI Starbase database. FC, fold change; OV, ovarian cancer; T, tumor; N, normal.

(Fig. 2D). The results of CCK-8 and BrdU assays indicated that cell proliferation decreased in the si-RHPN1-AS1 group in contrast to the blank groups and that there was no difference between NC and blank groups (Fig. 2E and F). After FCM was performed to observe cell apoptosis in the three groups, the results indicated that the number of apoptotic cells increased in the si-RHPN1-AS1 group compared with the blank group (Fig. 2G). Moreover, the wound-healing assay results indicated that silencing RHPN1-AS1 impaired the migration of SKOV3 and OVCAR3 cells (Fig. 2H and I). According to the outcome of the adhesion assay, the adherent cell number in the si-RHPN1-AS1 group was downregulated in contrast to the NC group or blank group in SKOV3 and OVCAR3 cell lines (Fig. 2J). Collectively, these results suggested that RHPN1-AS1 could enhance malignant growth in OC cells.

Effects of miR-485-5p on RHPN1-AS1. StarBase was employed to identify the binding sequences and the relationship between RHPN1-AS1 and miR-485-5p in OC cells (Fig. 3A). After performing luciferase reporter assay, it was observed that luciferase activities were reduced by 50% in SKOV3 and OVCAR3 cells co-transfected with the wild-type RHPN1-AS1-3'UTR plasmid and miR-485-5p mimics compared to the cells co-transfected with the mutated RHPN1-AS1-3'UTR plasmid and negative control. On the other hand, the luciferase activity in the cells co-transfected with mutant RHPN1-AS1-3'UTR plasmid and miR-485-5p mimics or negative control showed no statistical difference (Fig. 3B). The RIP assay results further confirmed that RHPN1-AS1 could merge with miR-485-5p (Fig. 3C). It was also found that miR-485-5p was downregulated by 60% in SKOV3 and OVCAR3 cell lines compared to the HOSEpiC cell line (Fig. 3D). Similarly, miR-485-5p decreased OC tissues by 60% compared to the adjacent normal tissues (Fig. 3E). Moreover, the correlation analysis revealed that RHPN1-AS1 had a negatively correlated expression pattern with miR-485-5p in OC tissues (Fig. 3F). Furthermore, to assess whether RHPN1-AS1 could regulate miR-485-5p expression, RHPN1-AS1 siRNAs were transfected into SKOV3 and OVCAR3 cell lines. The RT-qPCR results indicated that the expression of miR-485-5p in the si-RHPN1-AS1 group increased by 3-fold than that of the blank group (Fig. 3G). Taken together, the results revealed that a direct relationship existed between RHPN1-AS1 and miR-485-5p in OC cells.

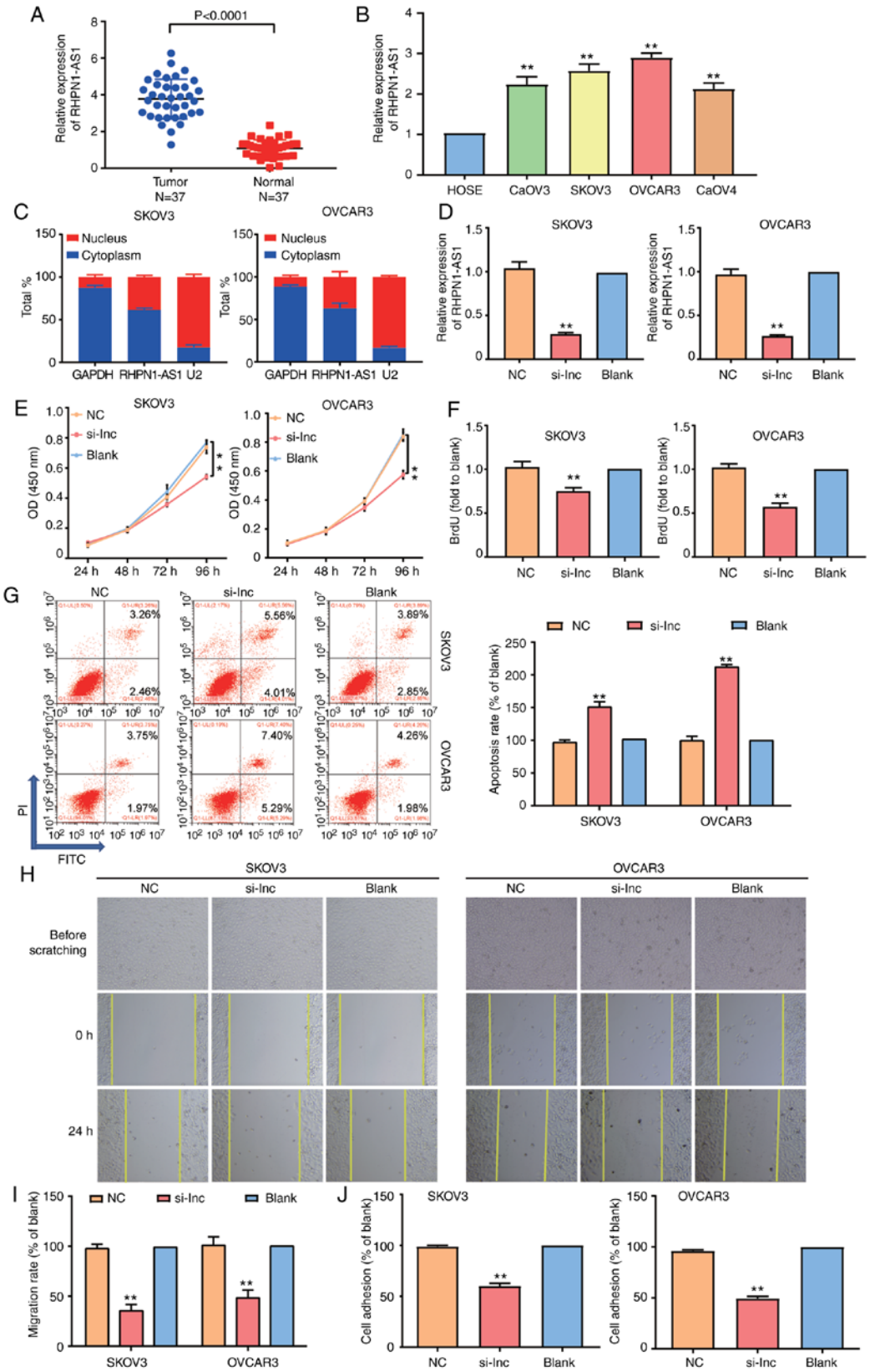

Figure 2. The function of RHPN1-AS1 in ovarian cancer. (A) RT-qPCR analysis revealed that the expression of RHPN1-AS1 was increased in OC tissues compared with adjacent healthy tissues. (B) RT-qPCR analysis revealed that the expression of RHPN1-AS1 was higher in OC cell lines than that in normal ovarian epithelial cells. (C) The location of RHPN1-AS1 in SKOV3 and OVCAR3 cell lines was analyzed by subcellular fractionation. (D) Transfection efficiency of SKOV3 and OVCAR3 cell lines with the transfection of si-RHPN1-AS1 (si-lnc group) was analyzed by RT-qPCR. (E) CCK-8 assay was used to observe the cell proliferation in the si-lnc, NC and blank groups. (F) BrdU assay was used to observe the cell proliferation in the si-lnc, NC and blank groups. NC, si-RHPN1-AS1 negative control; blank: Blank control. (G) Flow cytometry was employed to measure the cell apoptosis in si-lnc group, NC group and blank group. NC, si-RHPN1-AS1 negative control; blank: Blank control. (H and I) Wound healing assay was employed to measure the cell migration in si-lnc group, NC group and blank group. Original magnification, x100. (J) Cell adhesion assay was employed to measure the cell adhesion in si-lnc, NC and blank groups. NC, si-RHPN1-AS1 negative control; blank: Blank control. The cellular experiments were biologically repeated three times, and the data were presented as mean ± standard deviation (SD). **P<0.001 in contrast to blank group. NC, si-RHPN1-AS1 negative control; blank, blank control.

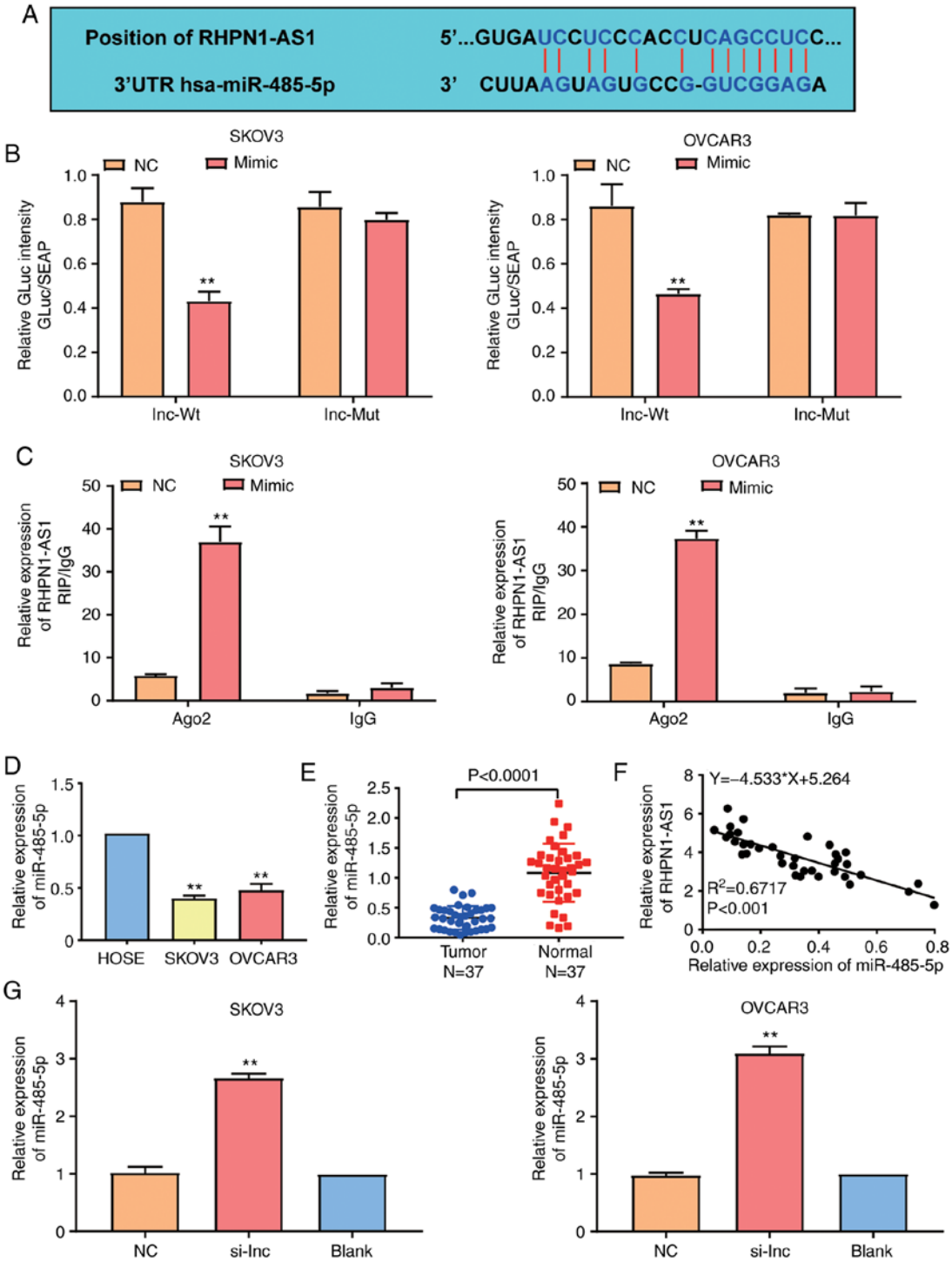

Figure 3. miR-485-5p was the downstream target gene of RHPN1-AS1. (A) The putative interacting sequences of RHPN1-AS1 and miR-485-5p was analyzed by StarBase 3.0. (B) Luciferase reporter assay was used to measure the target relationship between RHPN1-AS1 and miR-485-5p. NC, miRNA mimic negative control. (C) RIP assay was used to measure the interacting relationship between RHPN1-AS1 and miR-485-5p. NC, miRNA mimic negative control. (D) qRT-PCR analysis showed that the expression of miR-485-5p was downregulated in SKOV3 and OVCAR3 cell lines than that in normal ovarian epithelial cell. (E) RT-qPCR analysis showed that miR-485-5p was downregulated in SKOV3 and OVCAR3 cell lines than that in normal ovarian epithelial cells. (F) Pearson's correlation analysis revealed that RHPN1-AS1 had a negative relationship with miR-485-5p. (G) RT-qPCR analysis revealed that miR-485-5p was increased in si-RHPN1-AS1 group compared with NC group and blank group. NC, si-RHPN1-AS1 negative control. The cellular experiments were biologically repeated for three times, and the data were presented as mean ± standard deviation (SD). **P<0.001 in contrast to blank group.

Association between miR-485-5p andRHPN1-AS1. Several assays were performed to explore the regulatory association between RHPN1-AS1 and miR-485-5p in OC progression. Before the assay, the transfection efficiency was evaluated by RT-qPCR, and the results showed that transfection of si-RHPN1-AS1 significantly reduced the level of RHPN1-AS1 and miR-485-5p, while transfection of miR-485-5p inhibitor markedly decreased the level of miR-485-5p but had no effect on RHPN1-AS1 (Fig. S1). With the high transfection efficiency, the functional assays were then performed. The

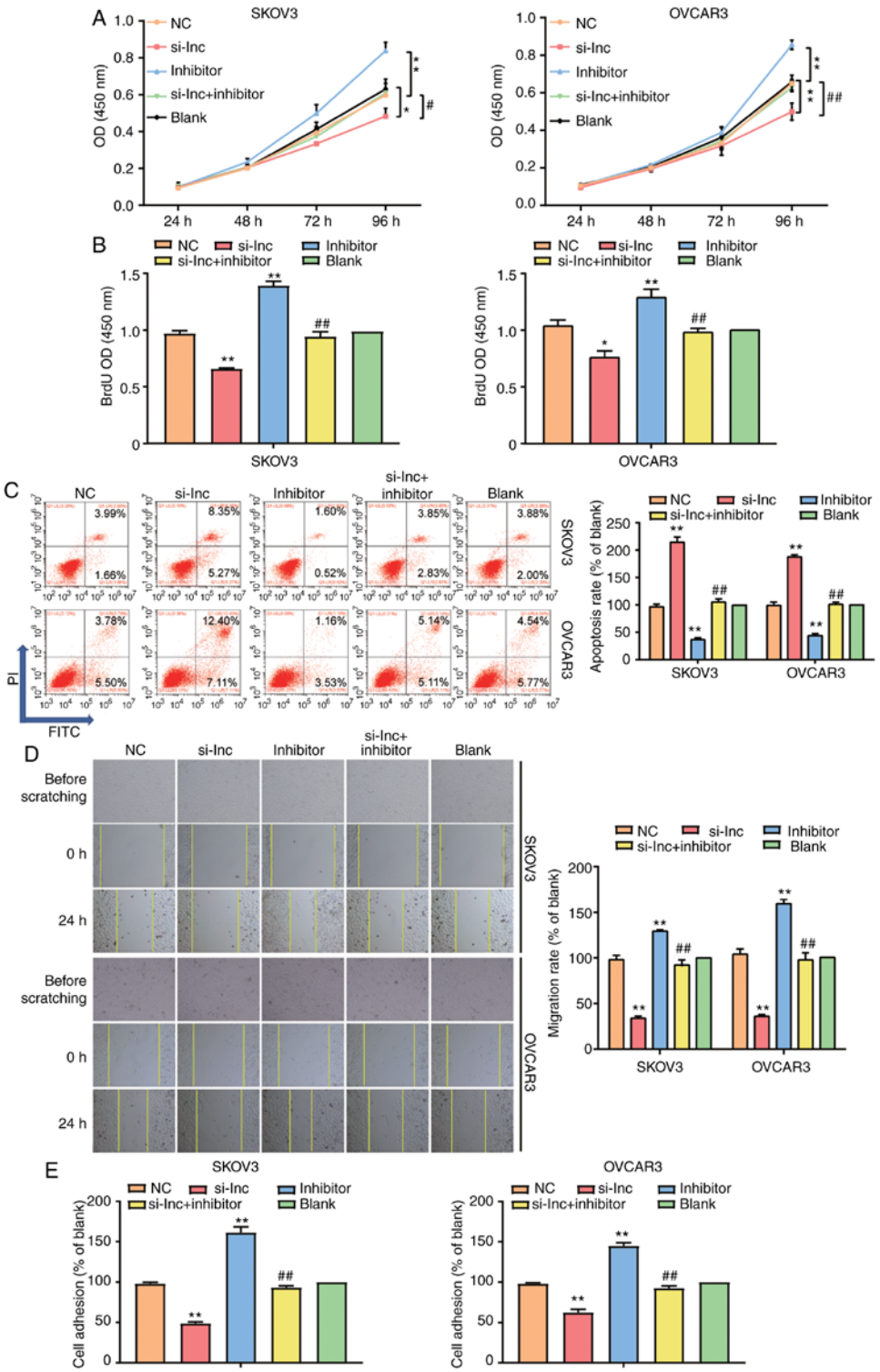

Figure 4. miR-485-5p weakened cell proliferation, migration and invasion while strengthened cell apoptosis in ovarian cancer cells which was regulated by RHPN1-AS1. (A) CCK-8 assay was used to observe the viability of SKOV3 and OVCAR3 cell lines after transfecting miR-485-5p inhibitor (inhibitor group), si-RHPN1-AS1 (si-lnc group), negative control (NC group, siRNA NC+inhibitor-NC) and co-transfecting miR-485-5p inhibitor and si-RHPN1-AS1 (si-lnc+inhibitor group) and untreated cells (blank group). (B) BrdU assay was used to observe the cell proliferation in the si-lnc, inhibitor, si-lnc+inhibitor, NC and blank groups. (C) Flow cytometry was employed to measure the cell apoptosis in the si-lnc, inhibitor, si-lnc+inhibitor, NC and blank groups. (D) Wound healing assay was employed to measure the cell migration in the si-lnc, inhibitor, si-lnc+inhibitor, NC and blank groups. Original magnification: x100. (E) Cell adhesion assay was employed to measure the cell adhesion in the si-lnc, inhibitor, si-lnc+inhibitor, NC and blank groups. The cellular experiments were biologically repeated for three times, and the data were presented as mean ± standard deviation (SD). *P<0.05, **P<0.001 contrast to blank group. $^{\#}$P<0.05, $^{\#\#}$P<0.001 in contrast to si-lnc group.

CCK-8 assay results showed that the miR-485-5p inhibitor enhanced cell viability, while si-RHPN1-AS1 impaired cell viability. When miR-485-5p inhibitor and si-RHPN1-AS1 were co-transfected, cell viability decreased considerably compared to the miR-485-5p inhibitor group (Fig. 4A). The BrdU assay outcome was similar to that of the CCK-8 assay in that

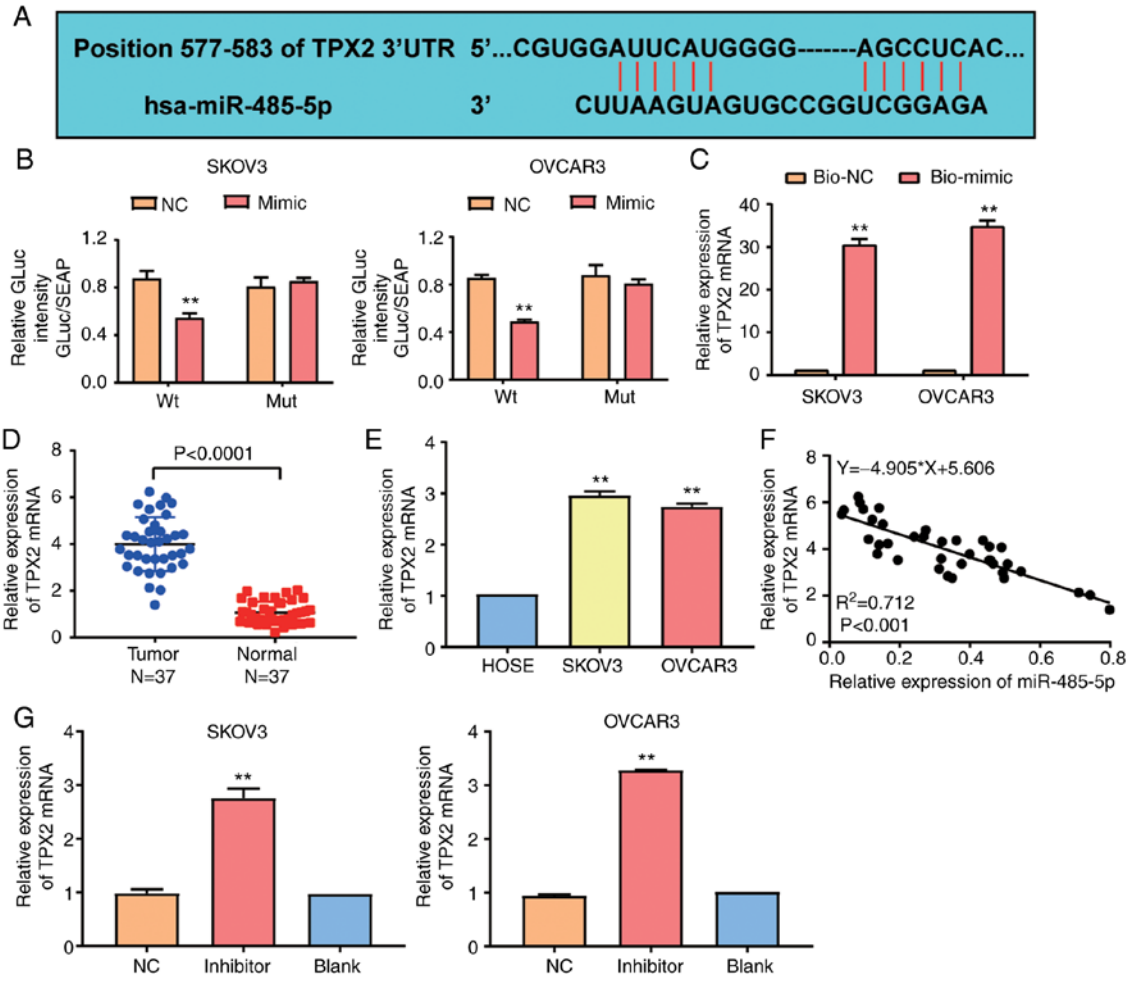

Figure 5. *TPX2* was the downstream target gene of miR-485-5p. (A) The competitive region sequences between miR-485-5p and *TPX2* was analyzed by TargetScan 7.2. (B) Luciferase reporter assay was used to measure the target relationship between miR-485-5p and *TPX2*. NC, miRNA mimic negative control. (C) RNA-pull down assay was used to measure the interacting relationship between miR-485-5p and *TPX2*. Bio-NC, bio-miRNA mimic negative control. (D) RT-qPCR analysis revealed that *TPX2* mRNA expression was higher in OC tissues than that in adjacent normal tissues. (E) RT-qPCR analysis showed that *TPX2* mRNA was higher in SKOV3 and OVCAR3 cell lines than that in normal ovarian epithelial cell by RT-qPCR. (F) Pearson's correlation analysis revealed that miR-485-5p had a negative relationship with *TPX2*. (G) RT-qPCR analysis revealed that *TPX2* was increased in miR-485-5p inhibitor group compared with blank group. NC, miRNA inhibitor negative control. The cellular experiments were biologically repeated for three times, and the data were presented as mean ± standard deviation (SD). **P<0.001 in contrast to blank group.

miR-485-5p inhibitor increased the proliferation of SKOV3 and OVCAR3 cell lines, while si-RHPN1-AS1 weakened cell proliferation. When miR-485-5p inhibitor and si-RHPN1-AS1 were co-transfected, the cell proliferation promotive effect of miR-485-5p inhibitor was completely reversed (Fig. 4B). In addition, the FCM results revealed that the cell apoptosis rate in the miR-485-5p inhibitor group decreased by 50% in contrast to the blank group but that the cell apoptosis rate increased by 2-fold in the si-RHPN1-AS1 group in contrast to the blank group in SKOV3 and OVCAR3 cell lines. After miR-485-5p inhibitor and si-RHPN1-AS1 were co-transfected, the suppression of cell apoptosis by miR-485-5p inhibitor was completely reversed (Fig. 4C). Furthermore, it was observed that the exogenous inhibition of miR-485-5p strengthened cell migration, whereas that of RHPN1-AS1 weakened the migration of SKOV3 and OVCAR3 cells. When both RHPN1-AS1and miR-485-5p were inhibited, the enhancement of cell migration by the miR-485-5p inhibitor was completely reversed (Fig. 4D). After cell adhesion assay was performed to measure the adhesion changes in SKOV3 and OVCAR3 cell lines, the results indicated that in the miR-485-5p inhibitor group, the adherent cell number was upregulated but that in the si-RHPN1-AS1 group, the adherent cell number was down-regulated compared to the blank group. After miR-485-5p inhibitor and si-RHPN1-AS1 were co-transfected, the increase in the adherent cell number by miR-485-5p inhibitor was completely reversed (Fig. 4E). These data revealed that RHPN1-AS1 could act on OC progression by negatively regulating miR-485-5p.

TPX2: The downstream target gene of miR-485-5p. TargetScan 7.2 was employed to identify the gene targeting miR-485-5p. The scanning results indicated that *TPX2* was the potential gene targeting miR-485-5p. The predicted competitive region sequences between miR-485-5p and *TPX2* 3'UTR are shown in Fig. 5A. Furthermore, the results of the luciferase reporter assay revealed that the luciferase activity was reduced by 40% in SKOV3 and OVCAR3 cells co-transfected with the wild-type *TPX2*-3'UTR plasmid and miR-485-5p mimic compared to cells co-transfected with the wild-type *TPX2*-3'UTR plasmid

and negative control. Nonetheless, no considerable difference was observed in cells co-transfected with mutant *TPX2*-3'UTR plasmid and negative control or miR-485-5p mimics (Fig. 5B). Similarly, the RNA-pull down assay findings indicated that miR-485-5p could bind to and interact with *TPX2* (Fig. 5C). With RT-qPCR, it was observed that the *TPX2* mRNA level in OC tissues was almost 4-fold higher than that in adjacent normal tissues (Fig. 5D). Similarly, the *TPX2* mRNA level was increased in SKOV3 and OVCAR3 cell lines compared to the HOSEpiC cell line (Fig. 5E). The correlation analysis also demonstrated a negatively correlated expression pattern between miR-485-5p and *TPX2* (Fig. 5F). To explore whether miR-485-5p could regulate *TPX2* expression, miR-485-5p inhibitor was transfected into SKOV3 and OVCAR3 cell lines, and the RT-qPCR results indicated that the *TPX2* mRNA level was upregulated in the miR-485-5p inhibitor group in contrast to the blank group (Fig. 5G). Overall, these data suggested that miR-485-5p could negatively regulate *TPX2*.

TPX2 strengthening ovarian malignancy was regulated by miR-485-5p. To explore the mechanism of *TPX2* related to miR-485-5p in depth, SKOV3 and OVCAR3 cell lines were transfected with miR-485-5p inhibitor, *TPX2* siRNA, negative control or co-transfected with miR-485-5p inhibitor and *TPX2* siRNA. After the protein level of *TPX2* in different grouped cells was evaluated using western blot analysis, the results revealed a 1.4-fold increase of *TPX2* in the miR-485-5p inhibitor group and at least a 40% decrease of *TPX2* in the si-*TPX2* group compared to the blank group. By contrast, it showed comparable *TPX2* expression in cells co-transfected with miR-485-5p inhibitor and *TPX2* siRNA and cells in the NC and blank groups (Figs. 6A and S2). The CCK-8 assay data showed that silencing *TPX2* reduced the viability of SKOV3 and OVCAR3 cells, while co-transfecting the miR-485-5p inhibitor completely reversed the changes caused by *TPX2* silencing (Fig. 6B). Similarly, the BrdU assay results showed that in contrast to blank groups, the cells in the si-*TPX2* group suppressed cell proliferation, which could be completely reversed by co-transfecting miR-485-5p (Fig. 6C). In addition, FCM findings revealed that the cell apoptosis rate in the si-*TPX2* group was upregulated by 2-fold; however, this effect could be completely reversed by co-transfecting miR-485-5p (Fig. 6D). Silencing *TPX2* was later found to decrease the migration capacity of SKOV3 and OVCAR3 cells; however, the miR-485-5p inhibitor could reverse the decrease (Fig. 6E). The adhesion assay results, on the other hand, showed that in the miR-485-5p inhibitor group, the adherent cell number was upregulated by 1.5-fold, whereas in the si-*TPX2* group, the adherent cell number was downregulated by 50%. After transfecting miR-485-5p inhibitor into the si-*TPX2* group, it was found that the increased adherent cell number caused by silencing *TPX2* was completely reversed (Fig. 6F). In sum, these results unveiled that after targeting *TPX2*, miR-485-5p could promote the proliferation, migration and invasion of OC cells and inhibit the apoptosis of OC cells.

Effect of RHPN1-AS1 on OC progression depended on TPX2. Western blot assay was performed to detect the protein level of *TPX2* in SKOV3 and OVCAR3 cells transfected with si-RHPN1-AS1 and/or miR-485-5p inhibitor. The results showed that *TPX2* decreased by 60% in OC cells transfected with si-RHPN1-AS1 compared to the control cells. However, this decrease was completely reversed by co-transfecting the miR-485-5p inhibitor (Fig. 7A). Subsequently, western blot assay was employed to examine the protein level of *TPX2* in SKOV3 and OVCAR3 cells transfected with si-RHPN1-AS1 and/or OE-*TPX2*, and the results showed that *TPX2* overexpression could significantly upregulate the protein level of *TPX2* and also effectively reversed the suppressive effect of si-RHPN1-AS1 on *TPX2* expression (Figs. 7B and S3). CCK-8 and BrdU assays were also performed to confirm the effect of RHPN1-AS1 on OC progression. The results of CCK8 assays revealed that silencing RHPN1-AS1 reduced the viability of SKOV3 and OVCAR3 cells; nevertheless, co-transfecting OE-*TPX2* reversed the reduction (Fig. 7C). Similarly, the BrdU assay results demonstrated that the weakened cell-proliferation ability induced by si-RHPN1-AS1 could be completely reversed by co-transfecting OE-*TPX2* (Fig. 7D). Collectively, these results revealed that the effect of RHPN1-AS1 on OC progression was dependent on *TPX2*.

Discussion

Our findings revealed that RHPN1-AS1 dominantly located in the cell cytoplasm was highly expressed in OC tissues and cell lines. In addition, RHPN1-AS1 enhanced the proliferation, migration and adhesion of OC cells but suppressed the apoptosis of OC cells. Apart from that, findings revealed that RHPN1-AS1 facilitated the tumorigenesis of OC by sponging miR-485-5p, which could regulate the proliferation, migration, adhesion and apoptosis of OC cells by targeting *TPX2*.

Previous research indicated that lncRNA RHPN1-AS1 was expressed in various types of cancer and was associated with tumorigenesis. For instance, in uveal melanoma, RHPN1-AS1 was overexpressed, thus promoting cell propagation, clone formation, cell migration and cell invasion (7). In another study, RHPN1-AS1 was upregulated in glioma, and it promoted cell propagation, migration and invasion by regulating miR-625-5p/REG3A directly (9). It was also previously reported that by targeting FGF2, RHPN1-AS1 influenced cervical carcinoma and exhibited a significantly negative relation with miR-299-3p to enhance cell propagation, migration, and invasion (10). Furthermore, RHPN1-AS1 accelerated cell proliferation and clone formation by sponging miR-4261 and targeting c-Myc in breast cancer (52). RHPN1-AS1 was utilized to predict poor prognosis in breast cancer patients due to its ability to enhance the growth of breast cancer cells by targeting the miR-6884-5p/ANXA11 pathway (53). Similarly, the upregulated RHPN1-AS1 in cell lines with colorectal carcinoma strengthened the propagation, migration and invasion of the tumor but weakened the apoptosis of the cancer by combining with miR-7-5p to stabilize O-GlcNAcylation transferase (OGT) (12).

In addition, the expression level of RHPN1-AS1 was higher in tissues with hepatocellular carcinoma than that in normal adjacent tissues (13). Findings of that study predicted shorter survival times in patients. RHPN1-AS1 overexpression also enhanced the proliferation and metastasis of hepatocellular

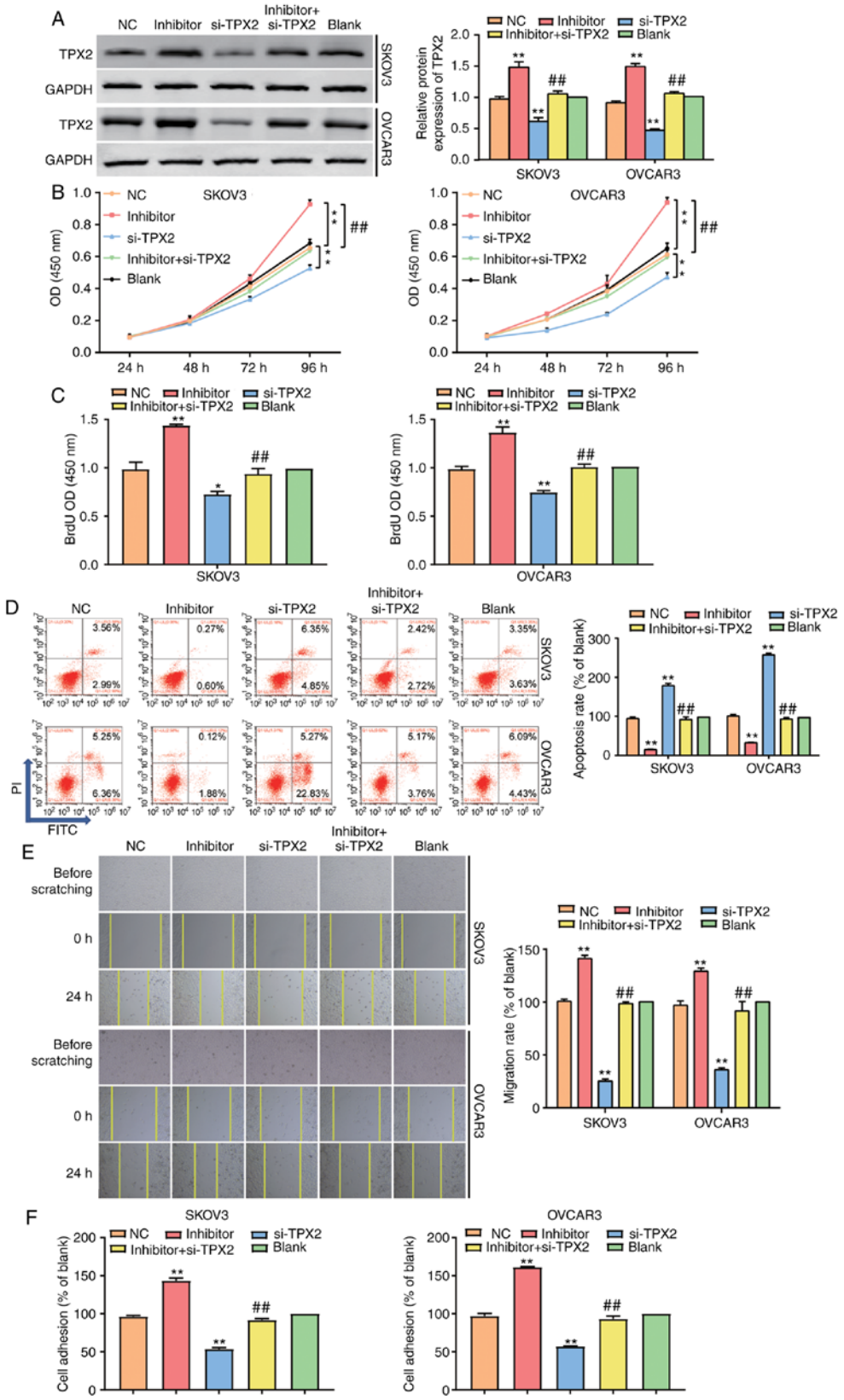

Figure 6. *TPX2* strengthened cell propagation, cell migration and invasion while weakened cell apoptosis in ovarian cancer cells which was regulated by miR-485-5p. (A) Western blot was employed to detect the protein level of *TPX2* in SKOV3 and OVCAR3 cell lines after transfecting miR-485-5p inhibitor (inhibitor group), si-*TPX2* (si-*TPX2* group), negative control (NC group, si-*TPX2* NC +inhibitor-NC) and co-transfecting miR-485-5p inhibitor and si-*TPX2* (inhibitor+si-*TPX2* group) and untreated cells (blank group). (B) CCK-8 assay was used to observe the cell proliferation in the si-*TPX2*, inhibitor, inhibitor+si-*TPX2*, NC and blank groups. (C) BrdU assay was used to observe the cell proliferation in the si-*TPX2*, inhibitor, inhibitor+si-*TPX2*, NC and blank groups. (D) Flow cytometry was employed to measure the cell apoptosis in the si-*TPX2*, inhibitor, inhibitor+si-*TPX2*, NC and blank groups. (E) Wound healing assay was employed to measure the cell migration in the si-*TPX2*, inhibitor, inhibitor+si-*TPX2*, NC and blank groups. Original magnification: x100. (F) Cell adhesion assay was employed to measure the cell adhesion in the si-*TPX2*, inhibitor, inhibitor+si-*TPX2*, NC and blank groups. The cellular experiments were biologically repeated for three times, and the data were presented as mean ± standard deviation (SD). *P<0.05, **P<0.001 in contrast to blank group. $^{\#\#}$P<0.001 in contrast to inhibitor group.

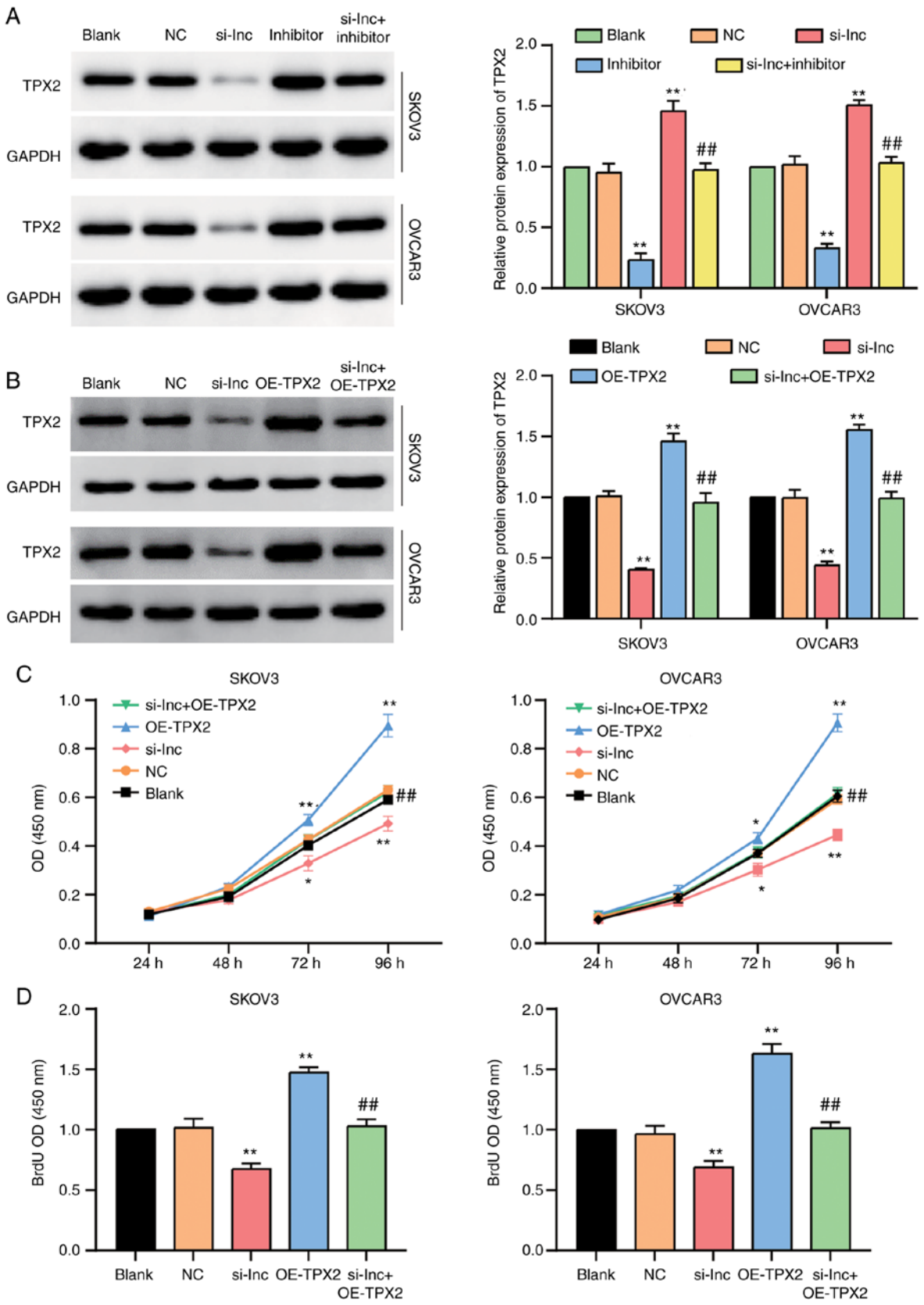

Figure 7. The regulation of RHPN1-AS1 to OC progression was dependent on *TPX2*. (A) Western blot was employed to detect the protein level of *TPX2* in SKOV3 and OVCAR3 cell lines with the transfection of si-RHPN1-AS1 (si-lnc group), miR-485-5p inhibitor (inhibitor group), co-transfecting si-RHPN1-AS1 and inhibitor (si-lnc+inhibitor group), negative control (NC group, siRNA NC+inhibitor-NC) and untreated cells (blank group). (B) Western blot was employed to detect the protein level of *TPX2* in SKOV3 and OVCAR3 cell lines with the transfection of si-RHPN1-AS1 (si-lnc group), OE-*TPX2* (OE-*TPX2* group), co-transfecting si-RHPN1-AS1 and OE-*TPX2* (si-lnc+OE-*TPX2* group), negative control (NC group, siRNA NC+empty vector) and untreated cells (blank group). (C) CCK-8 assay was used to observe the cell proliferation in si-lnc group, OE-*TPX2* group, si-lnc+OE-*TPX2* group, NC group and blank group. (D) BrdU assay was used to observe the cell proliferation in si-lnc group, OE-*TPX2* group, si-lnc+OE-*TPX2* group, NC group and blank group. The cellular experiments were biologically repeated for three times, and the data were presented as mean ± standard deviation (SD). *P<0.05, **P<0.001 in contrast to blank group. $^{\#\#}$P<0.001 in contrast to si-lnc group.

carcinoma (13). Another research reported that the high expression of RHPN1-AS1 had a significant correlation with advanced tumor metastasis stage, histologic grade and poor prognosis in hepatocellular carcinoma, which mainly resulted from its promotive action on cell proliferation, migration, and invasion through the miR-485/CDCA5 pathway (34). The sponging effect of RHPN1-AS1 on miR-485-5p has also been proved in another research that focused on hepatocellular carcinoma (33). Similar to the studies mentioned, our study verified that RHPN1-AS1 was overexpressed in OC, and this RNA may become a new biomarker in OC. Our research also showed that RHPN1-AS1 could not only promote cell proliferation, adhesion and migration but also suppress cell apoptosis in OC.

The potential role of miR-485-5p in the metastasis of multiple malignancies has been reported in the literature. For example, miR-485-5p was found to restrain mitochondrial respiration, cell invasion, cell migration and cell proliferation of breast cancer by directly suppressing PGC-1α (20). Similarly, miR-485-5p was downregulated in malignant melanoma cells and tissues compared to their corresponding controls (23). In non-small cell lung cancer, miR-485-5p could prevent cell growth, G0/G1 cell-cycle arrest, invasion and epithelial mesenchymal transformation (EMT) by downregulating IGF2BP2 (24). Moreover, lncRNA DSCR8 could reduce miR-485-5p by targeting the downstream molecule FZD7 to enhance the progression of hepatocellular carcinoma (21). In papillary thyroid cancer, the overexpression of LINC00460 and the downexpression of miR-485-5p were observed. An increase in LINC00460 expression enhanced cell proliferation, migration, invasion and EMT by targeting the miR-485-5p/Raf1 pathway (53). Similar to the results of previous research, the results of the present study showed a decrease in the expression of miR-485-5p in cells with OC. We also observed that miR-485-5p restricted cell proliferation, migration and adhesion, but facilitated cell apoptosis. Overall, these results offered more insights into the mechanism of OC development.

TPX2 is associated with aberrant expression and is highly expressed in various malignant tumors (55). In OC, TPX2 facilitated cell proliferation, invasion and migration but weakened cell apoptosis via the AKT signaling pathway (44). *TPX2* was also overexpressed in pancreatic cancer tissues and cell lines compared with normal controls; however, the exogenous silence of TPX2 suppressed cancerous growth (38). In addition, a report documented that TPX2 was highly expressed in tissues with gastric carcinoma compared to normal adjacent tissues and that it could strengthen cell proliferation, invasion and migration by enhancing EMT-related proteins (cdk2, cyclin D1, slug, MMP-9 and N-cadherin) and restraining E-cadherin (56). Findings of another study showed that, TPX2 was overexpressed in cervical carcinoma, thereby enhancing cell migration, invasion, and proliferation but inhibiting cell apoptosis and S-phase cell cycle arrest (57). In addition, this protein was found to be the downstream target gene of miR-8075, and it enhanced the proliferation, migration, and invasion of cervical cancer (42). The findings of this research were the same as those of previous studies: TPX2 was regulated by miR-485-5p, and it enhaned OC progression. This finding could aid the understanding of *TPX2* in OC and thus provide new ways of increasing the survival rate of OC patients.

Nevertheless, the current study has some limitations. We only designed *in vitro* cell experiments to determine the role of RHPN1-AS1, miR-485-5p and *TPX2* in OC progression. Put simply, *in vivo* experiments were not performed to verify our findings. Furthermore, we did not reveal how *TPX2* participated in OC development. Thus, we recommend that future research should verify our conclusion *in vivo* and investigate how *TPX2* influences OC tumorigenesis via potential signaling pathways such as AKT signaling pathway and EMT. In addition, due to the limitation of the microarray datasets used in this study, the DEGs at different stages were unable to be analyzed, which impedes the exploration of the more specific molecular basis of RHPN1-AS1 functioning in OC. In future work, we aim to identify other datasets or perform the microarray in different stages of OC to explore and analyze the DEGs, providing clues for the identification of specific biological significance of RHPN1-AS1 in OC.

In summary, our study suggested that RHPN1-AS1 could enhance OC progression by downregulating miR-485-5p and boosting *TPX2* expression. For this reason, we consider that RHPN1-AS1, miR-485-5p and *TPX2* may become new therapy targets for OC treatments.

Acknowledgements

Not applicable.

Funding

Not applicable.

Availability of data and materials

The datasets used and/or analyzed during the current study are available from the corresponding author on reasonable request.

Ethics approval and consent to participate

The study was approved by the Ethics Committee of Yantai Affiliated Hospital of Binzhou Medical University. All procedures performed in this study were in accordance with the 1964 Helsinki declaration. All the patients provided written informed consent.

Authors' contributions

SC was responsible for the conceptualization, methodology, investigation, data analysis, and manuscript preparation. CL was involved in methodology, investigation, visualization, resources, and manuscript preparation. CL and SC confirmed the authenticity of the data shown in the present manuscript. Both authors approved the final version of the study.

Patient consent for publication

Not applicable.

Competing interests

The authors declare that they have no competing interests.

References

1. Bray F, Ferlay J, Soerjomataram I, Siegel RL, Torre LA and Jemal A: Global cancer statistics 2018: GLOBOCAN estimates of incidence and mortality worldwide for 36 cancers in 185 countries. CA Cancer J Clin 68: 394-424, 2018.
2. Chen W, Zheng R, Baade PD, Zhang S, Zeng H, Bray F, Jemal A, Yu XQ and He J: Cancer statistics in China, 2015. CA Cancer J Clin 66: 115-132, 2016.
3. Lheureux S, Gourley C, Vergote I and Oza AM: Epithelial ovarian cancer. Lancet 393: 1240-1253, 2019.
4. Oza AM, Tinker AV, Oaknin A, Shapira-Frommer R, McNeish IA, Swisher EM, Ray-Coquard I, Bell-McGuinn K, Coleman RL, O'Malley DM, *et al*: Antitumor activity and safety of the PARP inhibitor rucaparib in patients with high-grade ovarian carcinoma and a germline or somatic BRCA1 or BRCA2 mutation: Integrated analysis of data from Study 10 and ARIEL2. Gynecol Oncol 147: 267-275, 2017.
5. Kim G, Ison G, McKee AE, Zhang H, Tang S, Gwise T, Sridhara R, Lee E, Tzou A, Philip R, *et al*: FDA approval summary: Olaparib Monotherapy in patients with Deleterious Germline BRCA-Mutated advanced ovarian cancer treated with three or more lines of chemotherapy. Clin Cancer Res 21: 4257-4261, 2015.
6. Shi X, Sun M, Liu H, Yao Y and Song Y: Long non-coding RNAs: A new frontier in the study of human diseases. Cancer Lett 339: 159-166, 2013.
7. Lu L, Yu X, Zhang L, Ding X, Pan H, Wen X, Xu S, Xing Y, Fan J, Ge S, *et al*: The long non-coding RNA RHPN1-AS1 promotes uveal melanoma progression. Int J Mol Sci 18: 226, 2017.
8. Qiu X, Lei Z, Wang Z, Xu Y, Liu C, Li P, Wu H and Gong Z: Knockdown of LncRNA RHPN1-AS1 inhibits cell migration, invasion and proliferation in head and neck squamous cell carcinoma. J Cancer 10: 4000-4008, 2019.
9. Cui P, Su J, Li Q, Xu G and Zhu N: LncRNA RHPN1-AS1 Targeting miR-625/REG3A promotes cell proliferation and invasion of glioma cells. Onco Targets Ther 12: 7911-7921, 2019.
10. Duan H, Li X, Chen Y, Wang Y and Li Z: LncRNA RHPN1-AS1 promoted cell proliferation, invasion and migration in cervical cancer via the modulation of miR-299-3p/FGF2 axis. Life Sci 239: 116856, 2019.
11. Zheng S, Lv P, Su J, Miao K, Xu H and Li M: Silencing of the long non-coding RNA RHPN1-AS1 suppresses the epithelial-to-mesenchymal transition and inhibits breast cancer progression. Am J Transl Res 11: 3505-3517, 2019.
12. Zheng W, Li H, Zhang H, Zhang C, Zhu Z, Liang H and Zhou Y: Long noncoding RNA RHPN1-AS1 promotes colorectal cancer progression via targeting miR-7-5p/OGT axis. Cancer Cell Int 20: 54, 2020.
13. Fen H, Hongmin Z, Wei W, Chao Y, Yang Y, Bei L and Zhihua S: RHPN1-AS1 drives the progression of hepatocellular carcinoma via regulating miR-596/IGF2BP2 Axis. Curr Pharm Des 25: 4630-4640, 2020.
14. Ding L, Wang L, Li Z, Jiang X, Xu Y and Han N: The positive feedback loop of RHPN1-AS1/miR-1299/ETS1 accelerates the deterioration of gastric cancer. Biomed Pharmacother 124: 109848, 2020.
15. Mattick JS: Non-coding RNAs: The architects of eukaryotic complexity. EMBO Rep 2: 986-991, 2001.
16. Bartel DP: MicroRNAs: Genomics, biogenesis, mechanism, and function. Cell 116: 281-297, 2004.
17. Li Z, Xu R and Li N: MicroRNAs from plants to animals, do they define a new messenger for communication? Nutr Metab (Lond) 15: 68, 2018.
18. Seok H, Ham J, Jang ES and Chi SW: MicroRNA target recognition: Insights from Transcriptome-wide non-canonical interactions. Mol Cells 39: 375-381, 2016.
19. Shao L, He Q, Liu Y, Liu X, Zheng J, Ma J, Liu L, Li H, Li Z and Xue Y: UPF1 regulates the malignant biological behaviors of glioblastoma cells via enhancing the stability of Linc-00313. Cell Death Dis 10: 629, 2019.
20. Lou C, Xiao M, Cheng S, Lu X, Jia S, Ren Y and Li Z: miR-485-3p and miR-485-5p suppress breast cancer cell metastasis by inhibiting PGC-1α expression. Cell Death Dis 7: e2159, 2016.
21. Wang Y, Sun L, Wang L, Liu Z, Li Q, Yao B, Wang C, Chen T, Tu K and Liu Q: Long non-coding RNA DSCR8 acts as a molecular sponge for miR-485-5p to activate Wnt/β-catenin signal pathway in hepatocellular carcinoma. Cell Death Dis 9: 851, 2018.
22. Ou R, Lv J, Zhang Q, Lin F, Zhu L, Huang F, Li X, Li T, Zhao L, Ren Y and Xu Y: circAMOTL1 Motivates AMOTL1 expression to facilitate cervical cancer growth. Mol Ther Nucleic Acids 19: 50-60, 2020.
23. Wu J, Li J, Ren J and Zhang D: MicroRNA-485-5p represses melanoma cell invasion and proliferation by suppressing Frizzled7. Biomed Pharmacother 90: 303-310, 2017.
24. Huang RS, Zheng YL, Li C, Ding C, Xu C and Zhao J: MicroRNA-485-5p suppresses growth and metastasis in non-small cell lung cancer cells by targeting IGF2BP2. Life Sci 199: 104-111, 2018.
25. Zhang Y, Hu J, Zhou W and Gao H: LncRNA FOXD2-AS1 accelerates the papillary thyroid cancer progression through regulating the miR-485-5p/KLK7 axis. J Cell Biochem 2018 (Epub ahead of print).
26. Duan J, Zhang H, Li S, Wang X, Yang H, Jiao S and Ba Y: The role of miR-485-5p/NUDT1 axis in gastric cancer. Cancer Cell Int 17: 92, 2017.
27. Chai Y, Du Y, Zhang S, Xiao J, Luo Z, He F and Huang K: MicroRNA-485-5p reduces O-GlcNAcylation of Bmi-1 and inhibits colorectal cancer proliferation. Exp Cell Res 368: 111-118, 2018.
28. Lin XJ, He CL, Sun T, Duan XJ, Sun Y and Xiong SJ: hsa-miR-485-5p reverses epithelial to mesenchymal transition and promotes cisplatin-induced cell death by targeting PAK1 in oral tongue squamous cell carcinoma. Int J Mol Med 40: 83-89, 2017.
29. Han DL, Wang LL, Zhang GF, Yang WF, Chai J, Lin HM, Fu Z and Yu JM: MiRNA-485-5p, inhibits esophageal cancer cells proliferation and invasion by down-regulating O-linked N-acetylglucosamine transferase. Eur Rev Med Pharmacol Sci 23: 2809-2816, 2019.
30. Wang FR, Xu SH, Wang BM and Wang F: miR-485-5p inhibits metastasis and proliferation of osteosarcoma by targeting CX3CL1. Eur Rev Med Pharmacol Sci 22: 7197-7204, 2018.
31. Gao F, Wu H, Wang R, Guo Y, Zhang Z, Wang T, Zhang G, Liu C and Liu J: MicroRNA-485-5p suppresses the proliferation, migration and invasion of small cell lung cancer cells by targeting flotillin-2. Bioengineered 10: 1-12, 2019.
32. Yang Y, Jiang Y, Wan Y, Zhang L, Qiu J, Zhou S and Cheng W: UCA1 functions as a competing endogenous RNA to suppress epithelial ovarian cancer metastasis. Tumour Biol 37: 10633-10641, 2016.
33. Zhang W, Han L, Xing P, Xing P, Liu B, Sun Z, Zhou W and Dong J: LncRNA RHPN1-AS1 accelerates proliferation, migration, and invasion via regulating miR-485-5p/BSG axis in hepatocellular carcinoma. Naunyn Schmiedebergs Arch Pharmacol 393: 2543-2551, 2020.
34. Zhang X, Yan Z, Wang L, Zhang S and Gao M: STAT1-induced upregulation of lncRNA RHPN1-AS1 predicts a poor prognosis of hepatocellular carcinoma and contributes to tumor progression via the miR-485/CDCA5 axis. J Cell Biochem, 2020 (Epub ahead of print).
35. Wittmann T, Boleti H, Antony C, Karsenti E and Vernos I: Localization of the kinesin-like protein Xklp2 to spindle poles requires a leucine zipper, a microtubule-associated protein, and dynein. J Cell Biol 143: 673-685, 1998.
36. Gruss OJ and Vernos I: The mechanism of spindle assembly: Functions of Ran and its target TPX2. J Cell Biol 166: 949-955, 2004.
37. Stewart S and Fang G: Anaphase-promoting complex/cyclosome controls the stability of TPX2 during mitotic exit. Mol Cell Biol 25: 10516-10527, 2005.
38. Warner SL, Stephens BJ, Nwokenkwo S, Hostetter G, Sugeng A, Hidalgo M, Trent JM, Han H and Von Hoff DD: Validation of TPX2 as a potential therapeutic target in pancreatic cancer cells. Clin Cancer Res 15: 6519-6528, 2009.
39. Tonon G, Wong KK, Maulik G, Brennan C, Feng B, Zhang Y, Khatry DB, Protopopov A, You MJ, Aguirre AJ, *et al*: High-resolution genomic profiles of human lung cancer. Proc Natl Acad Sci USA 102: 9625-9630, 2005.
40. Smith LT, Mayerson J, Nowak NJ, Suster D, Mohammed N, Long S, Auer H, Jones S, McKeegan C, Young G, *et al*: 20q11.1 amplification in giant-cell tumor of bone: Array CGH, FISH, and association with outcome. Genes Chromosomes Cancer 45: 957-966, 2006.
41. Wei P, Zhang N, Xu Y, Li X, Shi D, Wang Y, Li D and Cai S: TPX2 is a novel prognostic marker for the growth and metastasis of colon cancer. J Transl Med 11: 313, 2013.
42. Song T, Xu A, Zhang Z, Gao F, Zhao L, Chen X, Gao J and Kong X: CircRNA hsa_circRNA_101996 increases cervical cancer proliferation and invasion through activating TPX2 expression by restraining miR-8075. J Cell Physiol 234: 14296-14305, 2019.

43. Yan L, Li Q, Yang J and Qiao B: TPX2-p53-GLIPR1 regulatory circuitry in cell proliferation, invasion, and tumor growth of bladder cancer. J Cell Biochem 119: 1791-1803, 2018.
44. Tian Y, Liu LL, Guo DM, Wang Y, Zha WH, Li Y and Wu FJ: TPX2 gene silencing inhibits cell proliferation and promotes apoptosis through negative regulation of AKT signaling pathway in ovarian cancer. J Cell Biochem 119: 7540-7555, 2018.
45. Taherdangkoo K, Kazemi Nezhad SR, Hajjari MR and Tahmasebi Birgani M: miR-485-3p suppresses colorectal cancer via targeting TPX2. Bratisl Lek Listy 121: 302-307, 2020.
46. Livak KJ and Schmittgen TD: Analysis of relative gene expression data using real-time quantitative PCR and the 2(-Delta Delta C(T)) method. Methods 25: 402-408, 2001.
47. Li Y, Zheng F, Xiao X, Xie F, Tao D, Huang C, Liu D, Wang M, Wang L, Zeng F and Jiang G: CircHIPK3 sponges miR-558 to suppress heparanase expression in bladder cancer cells. EMBO Rep 18: 1646-1659, 2017.
48. Ma S, Rong X, Gao F, Yang Y and Wei L: TPX2 promotes cell proliferation and migration via PLK1 in OC. Cancer Biomark 22: 443-451, 2018.
49. Huang D, Chen J, Yang C and Wang M: TPX2 silencing mediated by joint action of microvesicles and ultrasonic radiation inhibits the migration and invasion of SKOV3 cells. Mol Med Rep 17: 7627-7635, 2018.
50. Zhao J, Yang T, Ji J, Zhao F, Li C and Han X: RHPN1-AS1 promotes cell proliferation and migration via miR-665/Akt3 in ovarian cancer. Cancer Gene Ther 28: 33-41, 2021.
51. Wang J, Ding W, Xu Y, Tao E, Mo M, Xu W, Cai X, Chen X, Yuan J and Wu X: Long non-coding RNA RHPN1-AS1 promotes tumorigenesis and metastasis of ovarian cancer by acting as a ceRNA against miR-596 and upregulating LETM1. Aging (Albany NY) 12: 4558-4572, 2020.
52. Zhu P, Li Y, Li P, Zhang Y and Wang X: c-Myc induced the regulation of long non-coding RNA RHPN1-AS1 on breast cancer cell proliferation via inhibiting P53. Mol Genet Genomics 294: 1219-1229, 2019.
53. Liang D, Liu H, Yang Q, He Y, Yan Y, Li N and You W: Long noncoding RNA RHPN1-AS1, induced by KDM5B, is involved in breast cancer via sponging miR-6884-5p. J Cell Biochem 2020 (Epub ahead of print).
54. Huang S, Zou C, Tang Y, Wa Q, Peng X, Chen X, Yang C, Ren D, Huang Y, Liao Z, *et al*: miR-582-3p and miR-582-5p suppress prostate cancer metastasis to bone by repressing TGF-β Signaling. Mol Ther Nucleic Acids 16: 91-104, 2019.
55. Morgan-Lappe SE, Tucker LA, Huang X, Zhang Q, Sarthy AV, Zakula D, Vernetti L, Schurdak M, Wang J and Fesik SW: Identification of Ras-related nuclear protein, targeting protein for xenopus kinesin-like protein 2, and stearoyl-CoA desaturase 1 as promising cancer targets from an RNAi-based screen. Cancer Res 67: 4390-4398, 2007.
56. Liang B, Zheng W, Fang L, Wu L, Zhou F, Yin X, Yu X and Zou Z: Overexpressed targeting protein for Xklp2 (TPX2) serves as a promising prognostic marker and therapeutic target for gastric cancer. Cancer Biol Ther 17: 824-832, 2016.
57. Chang H, Wang J, Tian Y, Xu J, Gou X and Cheng J: The TPX2 gene is a promising diagnostic and therapeutic target for cervical cancer. Oncol Rep 27: 1353-1359, 2012.